Cerebral Cortex January 2011;21:166–177
doi:10.1093/cercor/bhq073
Advance Access publication May 5, 2010

Fast Propagating Waves within the Rodent Auditory Cortex

Antonia Reimer[1], Peter Hubka[2], Andreas K. Engel[1] and Andrej Kral[1,2,3]

[1]Department of Neurophysiology and Pathophysiology, University Medical Center Hamburg-Eppendorf, 20246 Hamburg, Germany, [2]Department of Experimental Otology, Institute of Audioneurotechnology, Medical University Hannover, D-30625 Hannover, Germany and [3]School of Behavioral and Brain Sciences, University of Texas at Dallas, Richardson, TX 75083-0688, USA

Address correspondence to Andrej Kral, Institute of Audioneurotechnology (VIANNA), Medical University Hannover, Feodor-Lynen-Strasse 35, D-30625 Hannover, Germany. Email: a.kral@uke.de.

Central processing of acoustic signals is assumed to take place in a stereotypical spatial and temporal pattern involving different fields of auditory cortex. So far, cortical propagating waves representing such patterns have mainly been demonstrated by optical imaging, repeatedly in the visual and somatosensory cortex. In this study, the surface of rat auditory cortex was mapped by recording local field potentials (LFPs) in response to a broadband acoustic stimulus. From the peak amplitudes of LFPs, cortical activation maps were constructed over 4 cortical auditory fields. Whereas response onset had same latencies across primary auditory field (A1), anterior auditory field (AAF), and ventral auditory field and longer latencies in posterior auditory field, activation maps revealed a reproducible wavelike pattern of activity propagating for ~45 ms poststimulus through all cortical fields. The movement observed started with 2 waves within the primary auditory fields A1 and AAF moving from ventral to dorsal followed by a motion from rostral to caudal, passing continuously through higher-order fields. The pattern of propagating waves was well reproducible and showed only minor changes if different anesthetics were used. The results question the classical "hierarchical" model of cortical areas and demonstrate that the different fields process incoming information as a functional unit.

Keywords: anesthesia, cortical hierarchy, cortical organization, spatiotemporal pattern, traveling wave

Introduction

The brain represents features of sensory stimuli by the location of maximal excitation and by temporal features of neuronal responses. Provided that these 2 organizational principles act in coordinated fashion, they should generate a complex spatio-temporal pattern of evoked activity. Indeed, propagating cortical waves have been reported in the visual (Prechtl et al. 1997, 2000; Senseman and Robbins 1999; Sharon and Grinvald 2002; Roland et al. 2006; Benucci et al. 2007; Xu et al. 2007), somatosensory (Derdikman et al. 2003; Petersen et al. 2003), and motor cortex (Rubino et al. 2006) as well as in the olfactory bulb (Delaney et al. 1994). Propagating waves result when groups of neurons sequentially depolarize and hyperpolarize with small delays; the activity "travels" through the cortex according to the order and the degree of activation of areas. The vast majority of reports on cortical propagating waves applied optical imaging methods (Delaney et al. 1994; Prechtl et al. 1997; Sharon and Grinvald 2002; Derdikman et al. 2003; Petersen et al. 2003; Roland et al. 2006; Benucci et al. 2007; Xu et al. 2007).

In the auditory system, evoked propagating waves in the timescale of hundreds of milliseconds have been described and shown to propagate mainly within the isofrequency stripe in field primary auditory field (A1) (Bakin et al. 1996; Hess and Scheich 1996; Tsytsarev and Tanaka 2002; Tsytsarev et al. 2004). Using voltage-sensitive dyes, a cortical wave in the timescale of dozens of milliseconds was observed, again propagating within the isofrequency stripe (Song et al. 2006). This spread of activity has an anatomical correlate as thalamic afferents spread within the isofrequency stripe in a patchy pattern (Velenovsky et al. 2003; McMullen et al. 2005). On the other hand, both thalamocortical as well as corticocortical projections involve a significant extent of cortical tissue orthogonal to the isofrequency stripe (Lee and Winer 2008a, 2008b). Most likely, the propagation within the isofrequency band has been the consequence of pure tone stimulation used in previous studies, selected in the attempt to demonstrate cochleotopic cortical organization of the cortex and by that to verify the usefulness of optical imaging methods.

Optical imaging methods, especially intrinsic optical signals, have a high spatial resolution but hold the disadvantage of being insensitive to rapid changes in the temporal domain (Nelken et al. 2008; for dependence on wavelength, see Tsytsarev et al. 2008), thus providing temporally smoothed patterns of fast cortical activity. Voltage-sensitive dyes, although essentially toxic for neurons, allow determining faster changes of neuronal activity (Song et al. 2006; Tsytsarev et al. 2008). Differences in timing in the range of few milliseconds appear cardinal in cortical representation of the sensory world (Gourévitch and Eggermont 2007; Wei et al. 2008) and possibly in differentiating auditory objects (Nelken 2004). Consequently, direct electrophysiological investigations of propagating waves are required to investigate the true temporal scale over which they occur. In cochlear-implanted cats, a first electrophysiological study indeed observed a complex pattern of waves and "reflection" waves in fields A1 and anterior auditory field (AAF) evoked by electrical cochlear stimulation (Kral et al. 2009).

The present study demonstrates that evoked propagating waves can be observed also with acoustic stimuli, that they cover the whole auditory cortex, and that they travel in 2 directions: within A1 first dorsally, then also caudally and ventrally, and within AAF first dorsally, then ventrorostrally. Both activation fronts (from A1 and AAF) unify in passing through ventral auditory field (VAF) and end in posterior auditory field (PAF). To minimize a possible contamination of the wave by the anesthetics, 3 different anesthetic conditions with differently acting anesthetics were compared: 2 volatile anesthetics (isoflurane with and without nitrous oxide) and 1 nonvolatile anesthetic agent (ketamine). The study demonstrates that despite specific effects of the different anesthetics, cortical propagating waves constitute a stable phenomenon. The propagating waves demonstrated in this investigation further allow drawing conclusions about the hierarchical order of the cortical sensory areas in rat auditory cortex.

Materials and Methods

Animal Preparation

Sixteen male Brown Norway rats (287–373 g; Charles River) were included in this study. The experiments were performed with the approval of the German State Authority. All animals were initially anesthetized with a mixture of ketamine, xylazine, and atropine (ketamine 50 mg/kg, Graeub; xylazine 8 mg/kg, Bayer; atropine sulfate 0.25 mg/kg, B. Braun).

Animals were further divided into 3 groups. In a first group of rats (n = 8), anesthesia was maintained with isoflurane (0.6–1.3%; Abbott) in nitrous oxide (33%) and oxygen (66%). The second group (n = 4) received pure isoflurane (0.2–1.5%) in oxygen. Animals from both groups were artificially ventilated (Harvard Apparatus) through a tracheal cannula. A third group (n = 4) was anesthetized with intramuscular injections of ketamine (48.6–64 mg/kg, according to individual requirements), alternating hourly with 12.5 mg/kg ketamine, 2 mg/kg xylazine, and 0.00625 mg/kg atropine. These animals also received a tracheal cannula to facilitate breathing, but they were not artificially ventilated.

Depth of anesthesia was held at a constant and comparable level by a combination of several measures: testing for withdrawal reflex in response to interdigital twitch, control of a stable heart rate, registration of end-tidal CO_2 concentration, and the pressure in the ventilation system. A decrease in the level of anesthesia was noted by an increase in heart rate, an increase in end-tidal CO_2 concentration, the appearance of spontaneous breathing in ventilated animals, and the appearance of the paw withdrawal reflex. Similarly, opposite changes of these parameters signified an increased level of anesthesia. Rectal temperature was maintained at 37 °C via a feedback-controlled electric blanket (Otoconsult), and concentration of CO_2 in the expired air was monitored and held under 4% in ventilated animals (Datex Normocap; Datex Ohmeda). An infusion of Ringer and glucose (5 mmol/L) applied through a venous catheter served to maintain a constant level of body fluid (flow 1 mL/h; glucose 40%: B. Braun; Ringer solution: Delta-Pharma, Boehringer Ingelheim).

After fixating the animal in a snout holder, leaving the ears free from obstruction, the skull over the temporal cortex was trepanated (8 mm in rostrocaudal and 4 mm in dorsoventral direction) and the dura mater was resected. The cortex was kept moist by regular applications of Ringer solution. For documentation purposes, the cortex was photographed using a CCD camera attached to the microscope.

Stimulation and Recording

At the beginning of the experiments, 2 low-impedance Ag/AgCl electrodes (~5 kOhm) were positioned subcutaneously, one at the vertex in the midline in level with the interocular line and the other retroauricularly. Brainstem-evoked responses (filter 500 Hz to 5 kHz, amplification 500 000 times, 100 averages; amplifier: F1 Otoconsult) with click stimulation (condensation click, 50 μs duration) were used to determine the individual hearing thresholds. Only animals with normal hearing (brainstem-evoked response threshold <40 dB sound pressure level [SPL]) were included in further investigations. For cortical recordings, condensation clicks at SPLs 40 dB above the individual hearing threshold (determined by brainstem-evoked responses) were presented via calibrated loudspeakers (DT 48; Beyerdynamics). The loudspeakers were positioned approximately 2 mm in front of the left ear. At each position, 50 stimuli were applied (interstimulus interval: 513 ms).

After exposure of the right auditory cortex, a tungsten-in-glass microelectrode (impedance ~1 MΩ at 1 kHz; World Precision Instruments Inc.) was positioned epicortically and moved under microscopic control using a high-precision micromanipulator (TSE-Systems). The electrode just made contact with the brain surface but did not penetrate it. To map the auditory cortex, 80–220 positions per animal were investigated, their coordinates were registered, and the recording position was additionally marked on a photograph of the cortical surface. For recording, the electrode was attached to a recording system (Neuralynx Inc.). Signals were band-pass filtered (10 Hz to 10 kHz), amplified (40 dB), and recorded (100 ms pre- and 300 ms poststimulus) using a custom-made routine written in Matlab (MathWorks Inc.). Recordings were performed in a double-walled soundproof chamber (Acoustair).

Data Analysis

To analyze the temporal structure of cortical responses, 2 different measures were used: activity evaluated over all cortical recording positions (activation maps) and the time functions of activity (local field potentials [LFPs]) at specific cortical positions. Both these measures refer to the same phenomenon, spatiotemporal patterns of activity, from different viewpoints: the former is focused on time (activity over all cortical positions at one time shot) and the latter on cortical position (the temporal function of potential at one cortical position).

A custom-made Matlab program was used to compute the mean (evoked) LFP of each position. Evoked field potentials represent the time-invariant part of the cortical response and do not provide information on ongoing cortical activity. Onset and peak latencies used for plotting onset and peak maps were determined from the LFPs by an automatized routine written in Matlab. Onset latency was defined as the first latency at which the amplitude of the response exceeded the mean plus 4 times standard deviation of the absolute value of the signal before the response. Peak latency was the first positive local maximum of the signal after the onset, and the latency was plotted along the cortical location.

Activation Maps

Evoked responses of all positions were displayed simultaneously for one latency arranged in a matrix according to their coordinates. The amplitude of the potential was color-coded ("activation maps") and displayed as a movie sequence. To reveal the temporal progression of cortical activity irrespective of the amplitude of the responses, each individual LFP was additionally normalized to its maximum amplitude, giving relative LFPs (nLFPs). The propagating waves within such normalized activation maps were further processed.

Center of Gravity

To quantify the movement of the activity patterns, a function analogous to the center of gravity (COG) was computed at each time t, replacing the weight at each coordinate $[x, y]$ by the positive amplitudes of the relative LFP (nLFP) at the corresponding location:

$$\mathrm{COG}(t)_x = \frac{\sum_j x_j \cdot \mathrm{nLFP}(t)_j}{\sum_j \mathrm{nLFP}(t)_j},$$
$$\mathrm{COG}(t)_y = \frac{\sum_j y_j \cdot \mathrm{nLFP}(t)_j}{\sum_j \mathrm{nLFP}(t)_j}. \quad (1)$$

Here, $\mathrm{nLFP}(t)_j$ represents the positive amplitude of the nLFP recorded at position j at time t and x_j and y_j are the coordinates of the jth recording position. From these data, the velocity of the propagating wave was quantified using a simple measure: the positional change of the COG over time (Kral et al. 2009). For this calculation, the summed distance traveled by the COG was computed within a moving window of 5 ms and expressed in micrometer per millisecond. The determined onset of evoked LFPs (see above) occurred at 7 ms poststimulus. During the first 6.5 ms, the calculated position of the COG was consequently driven by spontaneous activity (was "random") and then "jumped" onto an initial position near the center of A1. This abrupt change, triggered by the first influence of the stimulus on the cortex, caused an erroneous peak in the propagation velocity at the stimulus onset. To avoid this, the COG values computed in the first 6.5 ms were considered as not evoked by the stimulus and were therefore blanked (set to 0).

Time Functions at Specific Cortical Positions

To investigate the time function at a specific location in the cortex, 9 positions with maximum amplitudes in P_a were selected from an area of 1 × 1 mm from most-responsive areas (hot spots) in each subject, and mean LFPs were then averaged over subjects (grand mean averages) and compared in millisecond-to-millisecond manner (2-tailed Wilcoxon–Mann–Whitney U test). Multiple comparisons were statistically accounted for by the false detection rate procedure (Benjamini

and Hochberg 1995). These data were used to investigate the functional organization of the auditory cortex in response to clicks.

Results

Activation Maps in Relation to Auditory Fields

Orientation on the cortex was based on vascular maps. Two regions with larger responses at short latencies were identified, a caudal and a rostral one (Figs 1 and 2). They were localized at positions corresponding to the primary auditory fields A1 and AAF, and both showed a reproducible relation to cortical vascular maps (cf. Tsytsarev et al. 2009). In what follows, the rostral spot will be referred to as rPA (rostral primary area corresponding to AAF) and the caudal spot as cPA (caudal primary area corresponding to A1). Despite a certain interindividual variability in their location (Fig. 2), they could be identified unequivocally in all animals and under all anesthetic conditions.

Morphology of LFPs

The absolute amplitudes of LFPs and their morphology differed at different cortical locations, generating activation maps (Fig. 1). LFPs were classified as P- or N-components based on polarity of peaks. LFPs differed in both latency and amplitude of the individual components P_a, N_b, and P_1 (Fig. 3). Later LFP components were less well reproducible (cf. Takahashi et al. 2005) and therefore excluded from further analyses.

There was a considerable variance in maximum amplitude of LFPs, whereas latencies were well reproducible (Table 1). Latencies of all 3 investigated components were shorter in rPA than in cPA, significantly for both P_a and N_b components (2-tailed Wilcoxon–Mann–Whitney test, $P < 0.001$). Amplitudes of LFPs were also significantly larger in rPA compared with cPA for both P_a and N_b (2-tailed Wilcoxon–Mann–Whitney test, $P < 0.001$). Grand mean averages computed and compared sample to sample in both these fields (after correction for multiple comparisons) showed significant differences between rPA and cPA mainly in P_a and N_b (2-tailed Wilcoxon–Mann–Whitney

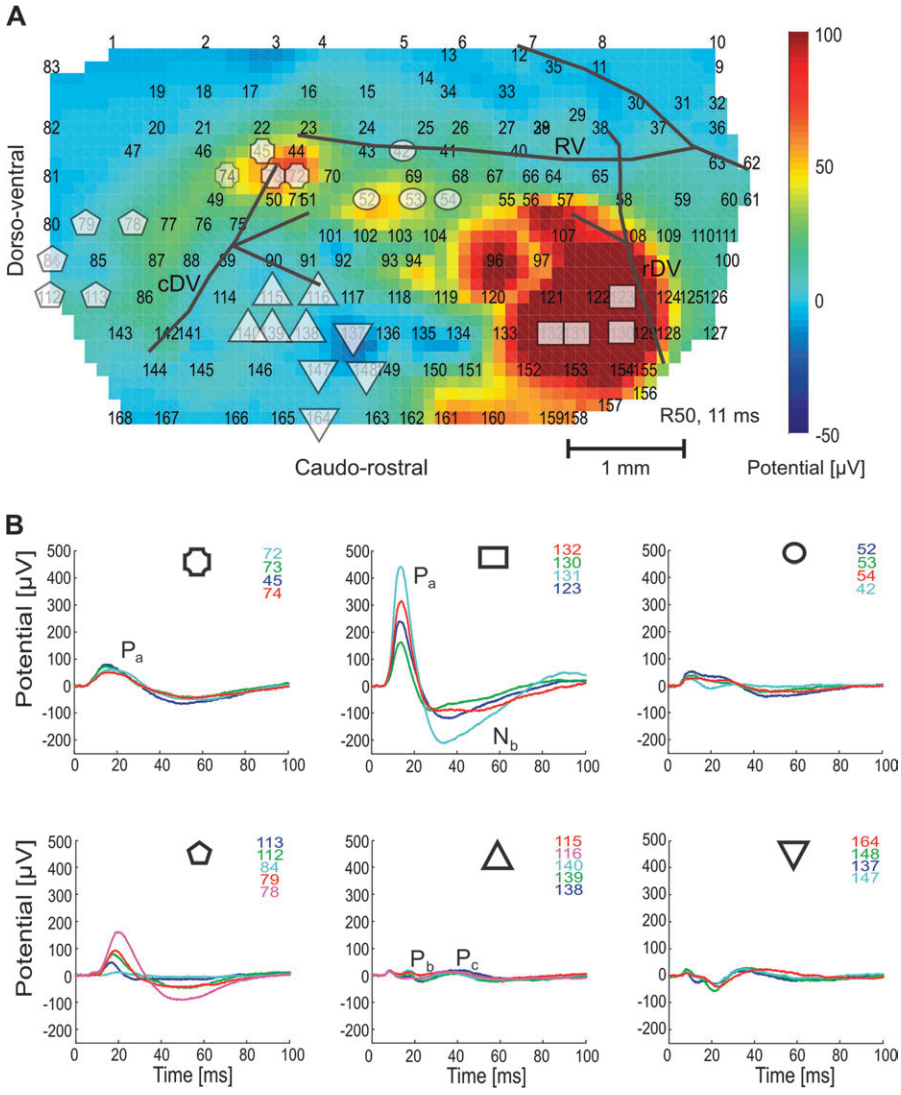

Figure 1. Classification of LFPs in an animal anesthetized with isoflurane/N_2O. (*A*) Map of absolute amplitudes of LFPs (color-coded) at 11 ms poststimulus. Lines indicate blood vessels, and symbols indicate the distribution of different types of LFPs as shown in (*B*). (*B*) Six different classes of LFPs, which differ in amplitude and latency of wave components. Numbers indicate position of recording corresponding to numbers in (*A*).

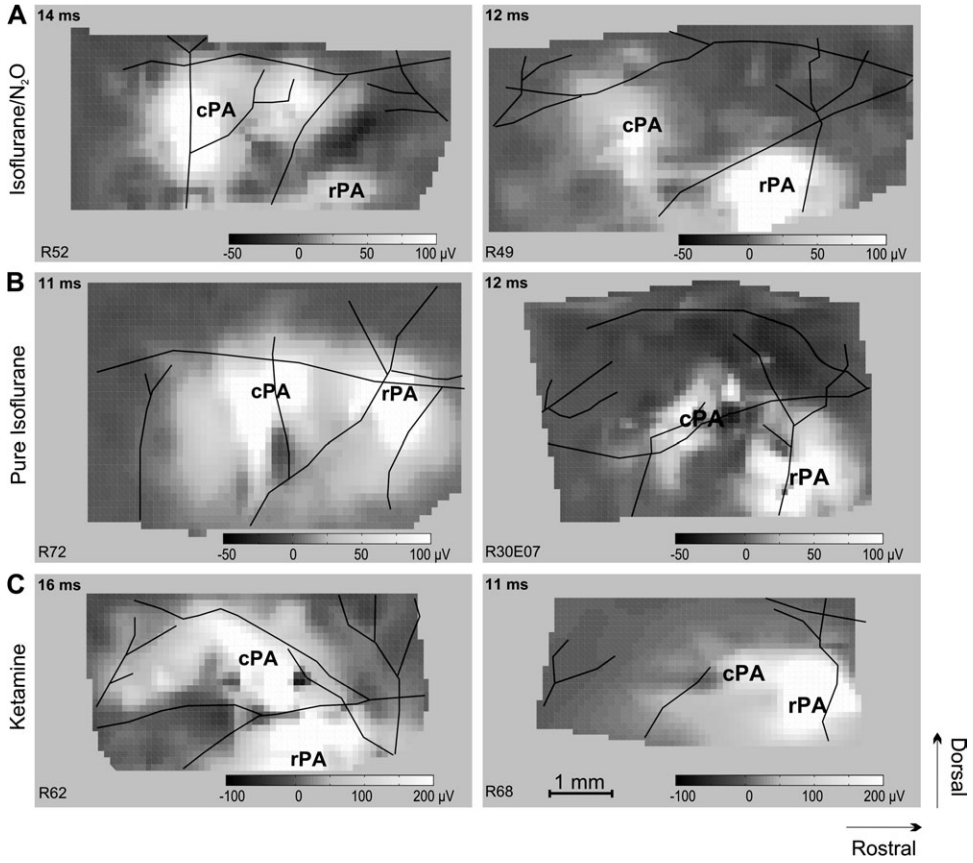

Figure 2. Maps of absolute LFP amplitudes showing the location and size of fields cPA and rPA in different anesthetic conditions. (*A*) Isoflurane/N_2O, (*B*) pure isoflurane, and (*C*) ketamine. Maps were taken at individual amplitude maxima in both fields, that is, between 11 and 16 ms poststimulus. Lines indicate the location of blood vessels.

Table 1
Mean latencies and potential amplitudes of LFP components P_a, N_b, and P_1 in cPA and rPA in different modes of anesthesia

Anesthesia	P_a		N_b		P_1	
	Latency (ms)	Amplitude (µV)	Latency (ms)	Amplitude (µV)	Latency (ms)	Amplitude (µV)
cPA						
Isofluorane/N_2O	19.43 ± 5.15	95.19 ± 67.13	51.57 ± 11.43	−61.53 ± 34.42	109.68 ± 15.88	15.22 ± 12.84
Isoflurane	17.24 ± 2.23	167.40 ± 122.00	47.24 ± 7.41	−118.61 ± 98.24	100.15 ± 11.32	34.77 ± 29.11
Ketamine	15.53 ± 2.86	152.06 ± 157.26	40.48 ± 11.38	−110.01 ± 105.42	85.39 ± 23.03	30.81 ± 33.60
rPA						
Isofluorane/N_2O	16.15 ± 2.56	176.70 ± 114.31	40.35 ± 13.06	−93.23 ± 52.75	99.15 ± 19.58	19.17 ± 14.48
Isoflurane	14.67 ± 1.85	141.97 ± 81.88	33.10 ± 8.72	−84.74 ± 52.81	71.56 ± 24.22	10.82 ± 19.42
Ketamine	14.84 ± 2.01	266.95 ± 173.87	29.70 ± 8.67	−161.17 ± 85.84	63.10 ± 23.80	29.96 ± 63.55

Note: Values were computed from 9 LFPs with maximum amplitudes in an area of 1 × 1 mm in cPA and rPA.

test, $P < 0.01$; Fig. 3*A*). The differences in morphology of the LFPs within these 2 regions remained significant in all 3 groups of animals, demonstrating that they were independent of the anesthetic condition.

Effects of Anesthetics

To investigate the effects of anesthetics on cortical LFPs, 3 types of anesthesia were used: isoflurane with N_2O, pure isoflurane, and ketamine. Despite the same depth of anesthesia as judged by other physiological parameters (see Materials and Methods), significant differences in heart rate were observed between the 3 groups (isoflurane/N_2O: 279 ± 20.5 bpm; pure isoflurane: 247 ± 28.5 bpm; ketamine: 220.3 ± 9.4 bpm; $P < 0.001$, Student's *t*-test).

Latencies and amplitudes of P_a, N_b, and P_1 (Table 1) were first compared between auditory fields within each group. The morphology of LFPs showed broader LFPs in cPA (i.e., latencies and amplitudes in medium range) and sharper LFPs in rPA (i.e., short latencies and large relative amplitudes; Fig. 3). Only with pure isoflurane, mean LFP amplitudes were higher in cPA than in rPA for both P_a and N_b. Fields cPA and rPA were regularly separated by a number of triphasic and negative LFPs (cf. Fig. 1), thus marking a distinct separation between fields.

Furthermore, we compared LFPs between corresponding fields of anesthetic groups. Shortest mean latencies for nearly all waves were found with ketamine (exception: P_a in rPA, where shortest latencies were found using pure isoflurane); longest latencies for all waves were recorded using isoflurane

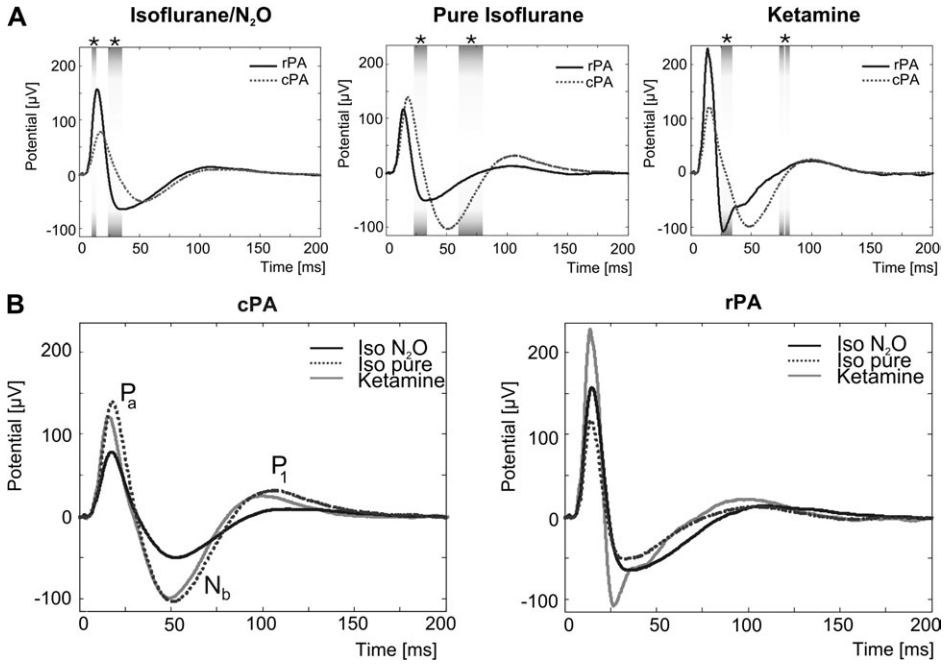

Figure 3. Grand mean averages of LFPs (*A*) in the fields cPA (dotted line) and rPA (straight line) in 3 anesthetic conditions. (*A*) Comparison of the LFPs for cPA and rPA. Left, isoflurane with nitrous oxide ($n = 8$); center, pure isoflurane ($n = 4$); right, ketamine intramuscularly ($n = 4$). Shaded bars and asterisks indicate significant variation between the combination of amplitude and latency of the 2 fields; these were obtained from 2-tailed Wilcoxon–Mann–Whitney test ($P < 0.01$). (*B*) Direct comparison of grand mean averages of LFP signals between different anesthetic agents in cPA and rPA.

and N_2O anesthesia (Table 1, Wilcoxon–Mann–Whitney test, $\alpha = 1\%$). In cPA, amplitudes in all peaks were highest using pure isoflurane and lowest using isoflurane and N_2O. In rPA, highest amplitudes in all 3 waves were found with ketamine (Fig. 3); peak amplitude was lowest with pure isoflurane in all components of the LFP (Table 1).

Overall, both ketamine and pure isoflurane showed similar effects on LFP morphology in field cPA, while LFP responses in rPA appeared similar using both types of isoflurane anesthesia. The most profound differences were observed between ketamine and isoflurane/N_2O, where LFPs differed significantly in both cPA and rPA in latencies of all wave components and in the amplitude of P_a and N_b in rPA (Table 1, Wilcoxon–Mann–Whitney test, $\alpha = 1\%$).

Spatial Patterns of Onset and Peak Latencies

To investigate the temporal sequence of cortical activation, the distribution of onset latencies of the LFPs over the auditory cortex was compared with the distribution of the peak latencies (Fig. 4*A*,*C*,*E*). In all anesthetic conditions, onset latencies were ~7 ms at a large portion of the cortical surface. However, there was a cortical region in the caudal most part of the auditory areas that showed systematically longer onset latencies in all anesthetic conditions (asterisk in Fig. 4*A*,*C*,*E*). This region corresponds in location to PAF.

Thalamic input evokes a response in the cortical neurons that cause the LFP to increase in amplitude to eventually reach a peak (i.e., maximum amplitude). When the latency–amplitude profiles of this peak were plotted over recording position (Fig. 4*B*,*D*,*F*), latencies of the responses markedly differed over the cortical areas. Longest peak latency was, similarly as onset latency, found in the most caudal area of the auditory cortex (asterisk, PAF). Overall, the amplitude–latency patterns were similar in isoflurane/N_2O group and ketamine but slightly different in the pure isoflurane group (cf. above). The shortest peak latencies were observed in the region located between cPA and rPA.

Patterns of Activation Waves

To allow the investigation of the spread of cortical activation irrespective of the absolute amplitude, a normalization of each LFP to its maximum amplitude was performed (cf. Kral et al. 2009). In the resulting activation maps, characteristic and reproducible wave patterns were observed within the first 45 ms (Fig. 5; see Supplementary Material for movies). The waves not only passed through the auditory regions rPA and cPA but also spread out beyond their borders. Despite some variability in detail, generally 3 phases of wave movements were observed: a rapid ventrodorsal movement (1), an extensive rostrocaudal movement (2), and a final motion in ventrodorsal direction at the caudal part of the cortex (3).

Within the first 7–12 ms, 2 primary waves arising from the ventral edge of the trepanated area moved into the areas cPA and rPA. According to their rostrocaudal location, they were named 1c and 1r. Frequently, a clear segregation between these waves could be seen within the normalized maps (marked by a dotted line in Fig. 5).

Secondary (reflection) waves followed at 13–20 ms. Again, as there were 2 separate wave fronts in cPA and rPA, the wave components were labeled 2c and 2r. These waves followed the primary waves in reversed direction and turned caudally thereafter. While the order of occurrence of these 2 components varied, 2r was always more dominant in appearance (see also Fig. 6 for trajectories of the COG). 2c and 2r united around 15–20 ms.

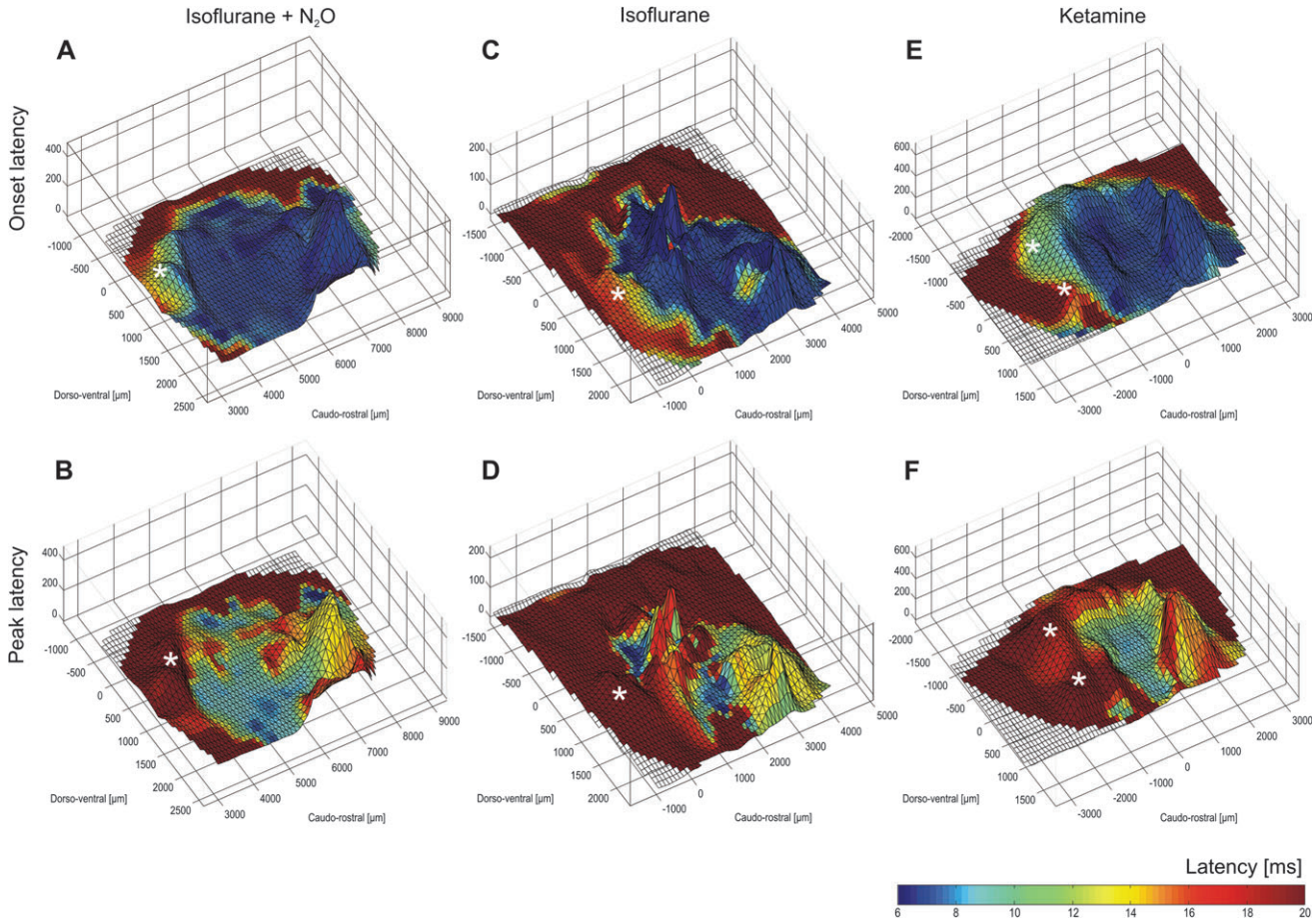

Figure 4. Onset latencies (*A*, *C*, *E*) and peak latencies (*B*, *D*, *F*) in different anesthetic conditions. (*A*, *B*) Isoflurane/N_2O, (*C*, *D*) pure isoflurane, and (*E*, *F*) ketamine. The area in the dimension of *x*/*y* corresponds to maps as shown in Figures 1 and 2, amplitudes (microvolts) are displayed as peaks and troughs along the z-axis, latencies (milliseconds) are color-coded as indicated by the color bar. An automated procedure was used to determine the first maximum >10 µV. Onset latencies are similar in cPA and rPA but longer in a caudal zone, probably PAF (marked by asterisk). Note that rPA has highest amplitudes and shortest peak latencies, followed by cPA; longest peak latencies appear in PAF.

A tertiary wave was observed at 20 (more frequently 25) to 30 ms poststimulus (labeled wave 3). It moved along the dorsoventral axis, mostly in dorsal direction. The remaining fluctuations occurring after 45 ms poststimulus were not well reproducible and were therefore not classified.

Despite generalizable wave pattern components, interindividual variability was also observed. In some animals, certain wave components were less well expressed or were delayed in time. Primary waves did not always occur simultaneously, and not always there were 2 distinct (i.e., spatially segregated) primary waves 1c and 1r (in part observable in Fig. 5*D*). Secondary waves 2c and 2r were present in every animal, although sometimes a delay of 2c was observed. Of all the 3 wave components, tertiary waves varied most and in some animals were not discernible at all.

Center of Gravity

From the above activation maps, the COG was computed and marked on the maps as a dot (Fig. 5). A trajectory of the COG was then computed and compared between different groups. For this purpose, trajectories were averaged after their realignment to the same mean position, obtaining a grand mean average (Fig. 6). In general, similar wave patterns at similar time spans were observed in all groups, leaving aside small interindividual variations.

Corresponding to the primary and secondary waves described above, COG trajectories showed an early rostrodorsal movement (corresponding to 1r and 1c), followed by a long caudal (corresponding to 2c and 2r) and a final rostrodorsal movement. After approximately 50–60 ms poststimulus, the COG trace remained in the center of the map with only slight fluctuations, complying with the observation that no further waves occurred after this time.

Using a sliding window (5-ms duration), the propagation velocity of the evoked waves was assessed from the location change of the COG over time (Kral et al. 2009). There were 3 distinct phases of acceleration in all 3 experimental groups (Fig. 7): a first acceleration (peak 1) at a window within 5–10 ms poststimulus, a second peak between 15–20 and 22–27 ms poststimulus, and a third peak between 40–45 and 55–60 ms poststimulus (Table 2 and Fig. 7). Highest velocities in the range of 100–200 µm/ms in accelerations 1 and 2 were found using pure isoflurane anesthesia, and slowest velocities were recorded for these peaks with isoflurane and N_2O (Table 2). While the average velocity of propagated waves hardly differed between experimental groups (~ 70 µm/ms), peak velocities did: earliest peak maxima were reached with ketamine and latest with isoflurane and nitrous oxide. Velocity in peak 2 was highest with pure isoflurane (187.64 µm/ms) and in peak 3 with ketamine (153.23 µm/ms) (cf. Table 2).

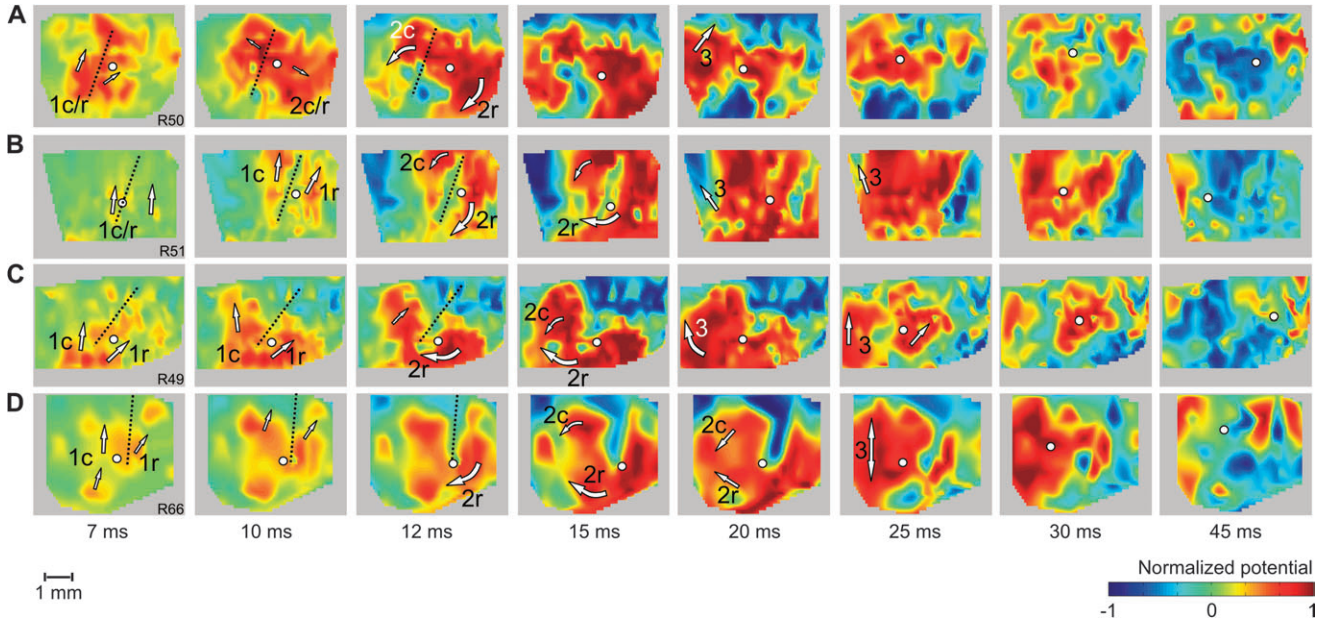

Figure 5. Activation maps normalized to maximum amplitude of each LFP; time slides at 7, 10, 12, 15, 20, 25, 30, and 45 ms poststimulus of 4 animals (anesthetized with isoflurane and N_2O) are shown. Arrows indicate the main movement of the leading edge of the wave taking place between one and the next picture. Numbers 1–3 label the main wave components as described in the text: 1c, 1r = primary waves (7–12 ms) in cPA and rPA, respectively; 2c, 2r = secondary waves in cPA and rPA, respectively (13–20 ms); 3 = tertiary wave (25–30 ms). Circles mark the map's COG; dotted lines show separation of waves between cPA and rPA.

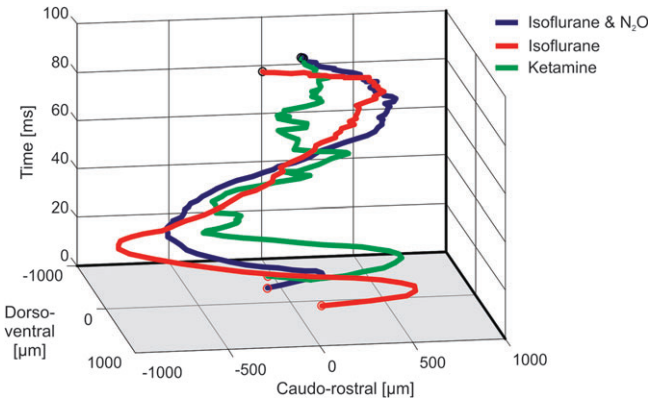

Figure 6. Trajectories of the movement of the COG in normalized maps. Grand mean averages of animals anesthetized with isoflurane/N_2O (blue), isoflurane (red), and ketamine (green) for the first 100 ms poststimulus. While the absolute distance traveled by COG differed between groups, the direction of movement was identical for the first 45 ms. A short rostral movement in the beginning was followed by the description of a large curve when the COG turned caudally, lasting for up to 20 ms. These observations correspond to the waves shown in Figure 5.

Latencies of peak 1 in the velocity profile were identical in all 3 experimental groups with the maximum acceleration occurring at 5–10 ms poststimulus, coinciding with components 1c and 1r (Fig. 5). There were, however, subtle differences in the exact latency of peak 2 between the experimental groups. Shortest latencies of peak velocity were recorded with pure isoflurane (15 ms for peak 2, 38 ms for peak 3), followed by ketamine (18 ms at peak 2, 52 ms at peak 3); with isoflurane and nitrous oxide, peak maxima occurred latest (21 ms for peak 2, 53 ms for peak 3). Velocity peak 2 coincided with the propagating wave components 2c and 2r described above (Fig. 5). Time windows of occurrence of velocity peak 3 were nearly identical with ketamine and isoflurane/N_2O anesthesia (ketamine: 52–57 ms, isoflurane/N_2O: 53–58 ms), but earlier using pure isoflurane anesthesia (38 ms, differences not significant). This velocity peak coincided with the disappearance of component 3.

Discussion

The present study demonstrates that LFP signals evoked by click stimulation formed a cortical propagating wave traveling within and across auditory areas in a stereotypical manner. These waves included components in dorsoventral as well as caudorostral dimensions and remained unchanged using different types of anesthesia. Finally, the sequence of cortical activation shown in this study (Fig. 8, see below) reveals a cortical "hierarchy" with fields A1 and AAF at the lowest level, field VAF at an intermediate level, and field PAF at the highest level. At the same time, however, several aspects of the data (e.g., propagation of the wave continuously through areal borders, same onset latencies of different fields) question the classical hierarchical model of cortical function.

Methodological Considerations

Click stimuli were used in the present investigations due to their short duration, very steep onset, and broadband spectrum. Especially the short duration represents an advantage compared with tonal stimulation, as the ongoing character of a tonal stimulus imposes an ongoing drive to the central auditory system, interfering with the dynamics of intrinsic cortical processes such as propagating waves. Therefore, clicks represent the optimal stimulus for the present investigations, being well suited for revealing cortical waves. However, clicks evoke a traveling wave along the cochlea (Carney and Yin 1988). This may impose a temporal sequence of activity progressing from high characteristic frequencies to low characteristic

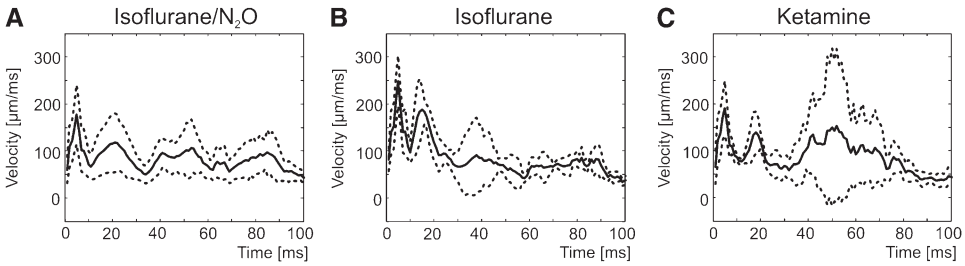

Figure 7. Grand mean averages of velocities of the movement of the COG. (*A*) Isoflurane/N_2O, (*B*): pure isoflurane, and (C) ketamine. Dotted lines show standard deviations.

Table 2
Peak velocities and time span of their occurrence of movement of COG in different anesthetic conditions; peaks 1–3 refer to peaks in Figure 7

	Peak 1		Peak 2		Peak 3	
	Time (ms)	Velocity (µm/ms)	Time (ms)	Velocity (µm/ms)	Time (ms)	Velocity (µm/ms)
Isoflurane/N_2O	5–10	177.20	21–26	117.60	53–58	190.11
Isoflurane	5–10	248.66	15–20	187.64	38–53	90.42
Ketamine	5–10	190.11	18–23	138.76	52–57	153.23

frequencies, which would explain a small part of the cortical wave. On the other hand, a previous study demonstrated that electrical stimulation of the auditory nerve via cochlear implants in cats also evokes a cortical propagating wave (Kral et al. 2009). As electrical stimulation of deaf ears does not generate a cochlear traveling wave, the evoked cortical wave must be the consequence of central processing. Here, a similar conclusion can be drawn from the same LFP onset latency at recording positions in the primary areas. The results of cortical microstimulation further support the conclusion (Song et al. 2006). Additionally, the timeline of the here-observed waves (5–30 ms) was of longer duration than the cochlear traveling wave. Taken together, the direct generation of the cortical wave by the cochlear traveling wave is improbable.

Positions in each animal were recorded sequentially. Thus, fluctuations in the physiological state of the animal, for example, depth of anesthesia, might have influenced the results. However, only the time-invariant portion of the signal was evaluated in the present study, as LFPs resulted from the average of 50 recordings. Indeed, LFP recordings were well reproducible, and the morphology of LFPs was more dependent on the cortical position than on time of recording (cf. Kral et al. 2009). Consequently, we do not consider state fluctuations as a significant confound in the present data.

To further exclude the anesthetic agent as the source of propagating waves, 3 different types of anesthesia were compared: volatile anesthesia with pure isoflurane, N_2O in addition to isoflurane (both including artificial ventilation), and intramuscular injections of ketamine (with spontaneous ventilation). Isoflurane has a widespread effect acting, for example, via increasing potassium conductivity by activation of extrasynaptic potassium channels (review in Franks 2008). It attenuates, among other areas, also activity in the auditory pathway and auditory cortex (Ori et al. 1986). Ketamine, on the other hand, is supposed to suppress thalamocortical activity (especially input from inferior colliculus and medial geniculate body) mainly via N-methyl-d-aspartate (NMDA) receptors but also γ-aminobutyric acid receptors (Anis et al. 1983; Mansbach 1991; Oye et al. 1992; Narimatsu et al. 2002; Freo and Ori 2004; Hevers et al. 2008; Franks 2008).

The present study has revealed a differential effect of anesthetics on the amplitude of LFPs within primary areas: isoflurane suppressed rPA to a greater extent than cPA. The effects of isoflurane observed here are in line with longer latencies and reduced amplitudes previously reported with isoflurane (Manninen et al. 1985; Sebel et al. 1986; Thiel et al. 1988; Thornton et al. 1992; Cheung et al. 2001; Santarelli, Arslan, et al. 2003; Santarelli, Carraro, et al. 2003; Franks 2008). Ketamine anesthesia showed reduced latencies of LFPs when compared with other anesthetics, corresponding well to previous reports (Massopust et al. 1972). Additionally, larger amplitudes were observed under ketamine both here and in previous studies (Kayama and Iwama 1972; Massopust et al. 1972; Wong and Jenkins 1974).

Our data demonstrate that N_2O, when combined with isoflurane, has a profound effect on cPA but less on rPA. The largest responses in cPA were found with pure isoflurane, both other anesthetics generated larger responses in rPA (largest with ketamine). This demonstrates a differential action of the anesthetics on the amplitude of LFPs in these 2 auditory fields and thus field-specific effects of the anesthetics. Adding N_2O to isoflurane makes the cortical responses more similar to those under ketamine, possibly due to N_2O action transmitted also by NMDA channels, thus resembling the action of ketamine (for review, see Franks 2008).

However, despite field-specific effects of anesthetics on amplitude maps, only minor effects of anesthetics on the spatiotemporal sequence of propagating waves were observed (Fig. 5; see also Supplementary Material). In general, the addition of N_2O to isoflurane, although increasing component latencies, had also a beneficial experimental effect: it allowed using lower isoflurane concentrations and allowed a better control of anesthesia.

The method of quantifying the velocity of propagating waves using the COG is in many cases inaccurate, especially when 2 wave fronts propagate into opposite directions. In such situations, the true velocity is underestimated. However, COG provides a simple way of quantifying the mean overall propagation velocity and allows comparison to a previous study (Kral et al. 2009). The results obtained correspond well

to the velocities determined by other methods (Kubota et al. 1997; Benucci et al. 2007; Xu et al. 2007).

Functional Organization of the Auditory Cortex

Similar hot spots to cPA and rPA were observed with click stimulation and voltage-sensitive dyes (Tsytsarev et al. 2009). They correspond to primary fields A1 and AAF: First, their latency corresponds to response latencies in these fields, as well as their relation to the vascular map (Kalatsky et al. 2005; Takahashi et al. 2005; Polley et al. 2007). Second, the response amplitudes of LFPs were larger in rPA than in cPA and had a steeper onset and slightly shorter latency, which again corresponds to AAF when compared with A1 (Takahashi et al. 2005). Another aspect for the distinction of auditory fields was the shape of LFPs, which is characteristic for the individual cortical areas. In rPA, latencies of LFP peaks were shorter and amplitudes larger than in cPA, again corresponding to AAF and A1 (Shaw 1988, 1990; Barth and Di 1990, 1991; Takahashi et al. 2005). The position of other cortical fields was then extrapolated from the vascular map and the mutual relation of these fields to A1 and AAF (Fig. 8; cf. Polley et al. 2007).

Propagating Waves

The present study shows a reproducible propagating wave in rat auditory cortex in response to a broadband auditory stimulus with very steep onset and short duration. The wave had a reproducible direction, speed, and duration and was initiated from a reproducible position in all investigated animals. Similar waves have been described in other cortical regions (visual cortex: Prechtl et al. 1997, 2000; Senseman and Robbins 1999; Sharon and Grinvald 2002; Roland et al. 2006; Benucci et al. 2007; Xu et al. 2007; somatosensory cortex: Derdikman et al. 2003; Petersen et al. 2003; motor cortex: Rubino et al. 2006; olfactory bulb: Delaney et al. 1994). Although a general propagation pattern was found in all animals examined, there was also some variability in the occurrence of one or more components of the propagating wave. This is not surprising, given that the tonotopic arrangement of the early cortical fields can in detail also differ substantially between different animals (Sally and Kelly 1988).

Most extensive work on propagating waves has been done on the visual cortex using optical imaging (Prechtl et al. 1997, 2000; Senseman and Robbins 1999; Sharon and Grinvald 2002; Roland et al. 2006; Benucci et al. 2007; Xu et al. 2007). A compression and reflection wave pattern has recently been described in fields V1/V2 after visual stimulation with a shifting grating in deeply anesthetized animals (Xu et al. 2007). The propagating wave described by Xu et al. occurred with a latency of ~100 ms poststimulus and had a duration of approximately 120 ms. The visual system, however, typically exhibits long onset latencies due to a slow retinal transduction process. In the auditory cortex, voltage-sensitive dyes demonstrated a propagating wave restricted to the isofrequency band with latency of ~20 ms and duration of ~20 ms applying tonal stimulation (Song et al. 2006). The present manuscript, applying electrophysiological methods, demonstrated a wave with even a shorter latency but comparable duration. The differences in latency most likely result from an indirect recording of activity in the previous studies. However, cortical propagating waves evoked by intracortical electrical stimulation in a voltage-sensitive dye study had a very short latency of only ~2–4 ms (Song et al. 2006; cf. Tsytsarev et al. 2008).

Previous studies using optical methods revealed a propagation of the cortical wave within the isofrequency domain (Harrison et al. 2000; Versnel et al. 2002; Ojima et al. 2005; Song et al. 2006). No significant components parallel to the tonotopic axis were described. The first study performed with electrophysiological methods and cochlear implant stimulation in cats clearly demonstrated a propagation of the wave from the high-frequency portion of A1 and AAF into the low-frequency regions of both fields (Kral et al. 2009). The present study, using acoustical stimulation in rats, also demonstrated rostrocaudal components of the waves.

The observed propagating velocities of up to ~200 μm/ms are concurrent with reports based on optical imaging, for example, velocities around 200 μm/ms for horizontal propagation in brain slices (Kubota et al. 1997), 380 ± 100 μm/ms in the auditory cortex (Song et al. 2006), and around 300 μm/ms (Benucci et al. 2007) and 50–70 μm/ms (Xu et al. 2007) in the visual cortex. The results of the present investigation were thus in the same range as in previous studies. Also, the velocity of action potentials in horizontal fibers is up to 500 μm/ms (Nowak and Bullier 1998), comparable with the present result. Cortical inhibition (Shamma and Symmes 1985; Calford and Semple 1995; Sutter et al. 1999) could have influenced the direction and the speed of the propagating wave. The presence of minima in propagation velocities has been attributed to action of inhibition that appears to slow down the propagation waves (Xu et al. 2007). Similarly as in the cited study, slowing down of the waves occurred when they reached areal borders: first, when waves 1r and 1c reached the presumed dorsal

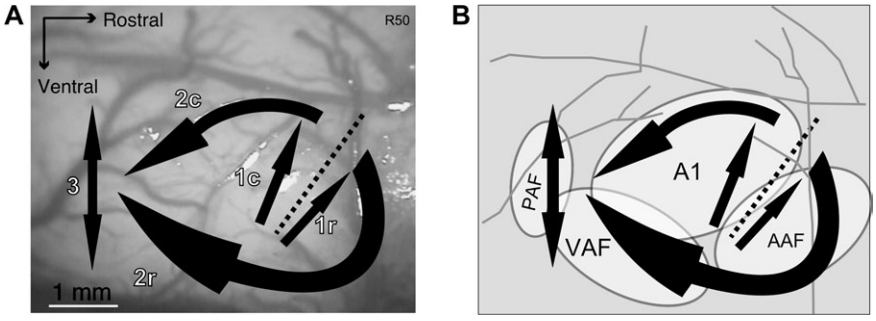

Figure 8. Movement of propagating waves projected onto a photograph of the cortical surface (*A*, right temporal cortex) and onto a scheme of rat auditory fields with vessel contours outlined (*B*, modified from Polley et al. 2007). 1c, 1r = Primary waves (7–12 ms) in cPA and rPA, respectively; 2c, 2r = secondary waves in cPA and rPA, respectively (13–20 ms); 3 = tertiary wave (25–30 ms).

border of A1 and AAF (after 10 ms poststimulus) and second when waves 2c and 2r reached the presumed ventrocaudal border of A1 and the caudal border of AAF/VAF. The third acceleration occurred when spots of activity disappeared. More research is required to correlate the slow-down regions with functionally defined area borders.

Relation to Functional Cortical Architecture

The cortical wave observed here was complex and reflected the sequential activation of cortical regions belonging to different auditory fields. As onset latency can be considered the consequence of the thalamic input, with the exception of the caudal most region (PAF) the cortical areas appear to get simultaneous direct input from the lemniscal thalamus over the whole extent of the areas. The region corresponding to VAF did not have a longer onset latency, indicating that at least a certain portion of the thalamic input to this field originates in lemniscal thalamic nuclei. The fact that onset responses appeared with nearly identical latency in the majority of cortical areas indicates that thalamic input is not a likely generator of the propagating wave. The wave could be the consequence of horizontal cortical interactions within the supragranular layers (Kubota et al. 1997; Nowak and Bullier 1998) and as such would possibly represent a substrate for integration of sensory features within the primary fields. When investigating nonnormalized activation maps, the responses reached high amplitudes only at certain positions within the primary fields (Fig. 4), as described also by Tsytsarev et al. (2009). Consequently, only in some positions, neurons are stimulated strongly; however, subthreshold input and modulation can be imposed over long cortical distances and many fields via the cortical wave. Since LFPs represent the summed postsynaptic activity, we cannot clearly delineate the region of the cortex that has been excited over spiking threshold. However, it is probable that it will significantly overlap with the hot spots described in not-normalized amplitude maps.

Propagating waves are also the consequence of the timing of neural activity within and between different cortical areas. In this sense, they provide a substrate for integration of activity in different cortical fields (Contreras 2007). The propagation of activity from "early" to "late" cortical areas, in correspondence with the proposal of cortical hierarchy, could be directly observed here. However, such propagation of activity can most likely be observed only with short-duration stimuli with steep onset. We assume that using stimuli with smeared onset or ongoing stimuli, this propagation wave will be modified by the ongoing sensory input. Also, the propagating wave cannot be observed without eliminating amplitude maps as it is obscured by amplitude differences in the responses caused by the overlaid representation of different acoustic features at different cortical positions (review in Schreiner and Winer 2007). One possible consequence of the present findings is that the absolute amplitude map reveals the "winner population" of neurons within the field (cf. Benucci et al. 2007), while the normalized map additionally reflects the propagation of subthreshold activity. It represents the substrate for integration of features represented at distant cortical locations. Additionally, the propagating wave demonstrates the predominant local connectivity of cortical neuronal networks (Ermentrout and Kleinfeld 2001).

We observed the activity to flow from early areas to the presumed late areas (Fig. 8), indicating a progress of activity within the functional cortical hierarchy of the fields. The results in fact correspond to previous unit data (Polley et al. 2007) and put the primary fields A1 and AAF at the lowest stage of cortical processing, followed by VAF (and suprarhinal auditory field if existent) to finally reach the highest stage in PAF. Data on binaural sensitivity are required to elucidate whether or not the rat PAF is a homolog of the feline PAF (Rouiller et al. 1991; Read et al. 2002; Winer and Lee 2007). However, the continuous nature of the propagating wave (flowing continuously through the areal borders) together with the simultaneity of the onset latency at different fields rise doubts on the classical concept of cortical hierarchy and emphasize that auditory fields together represent a functional unit. A hierarchical model may thus be a very simplified view on cortical function.

Conclusions

The present study demonstrates a stereotypical cortical propagating wave within the rat auditory cortex using electrophysiological methods. It shows that although cortical hierarchy has been traditionally concluded from differences in response latencies, onset latencies of LFPs do not demonstrate such a difference along A1, AAF, and VAF. Additionally, comparing the observed activation patterns with amplitude maps of LFPs demonstrates that the cortex integrates the incoming information over the whole auditory cortex in the form of a propagating wave flowing continuously through areal borders to establish the final amplitude (firing) pattern.

Funding

In part by Deutsche Forschungsgemeinschaft (Kr 3370/1-1 and 1-2).

Supplementary Material

Supplementary material can be found at: http://www.cercor.oxfordjournals.org/.

Notes

We thank D. Bystron for excellent technical assistance and her contribution to the experimental part of this manuscript and Dr J. Tillein for critical comments on a previous version of the manuscript. *Conflict of Interest*: None declared.

References

Anis NA, Berry SC, Burton NR, Lodge D. 1983. The dissociative anaesthetics, ketamine and phencyclidine, selectively reduce excitation of central mammalian neurones by N-methyl-aspartate. Br J Pharmacol. 79:565–575.

Bakin JS, Kwon MC, Masino SA, Weinberger NM, Frostig RD. 1996. Suprathreshold auditory cortex activation visualized by intrinsic signal optical imaging. Cereb Cortex. 6:120–130.

Barth DS, Di S. 1990. Three-dimensional analysis of auditory-evoked potentials in rat neocortex. J Neurophysiol. 64:1527–1536.

Barth DS, Di S. 1991. The functional anatomy of middle latency auditory evoked potentials. Brain Res. 565:109–115.

Benjamini Y, Hochberg Y. 1995. Controlling the false discovery rate: a practical and powerful approach to multiple testing. J R Stat Soc B. 57:289–300.

Benucci A, Frazor RA, Carandini M. 2007. Standing waves and traveling waves distinguish two circuits in visual cortex. Neuron. 55:103–117.

Calford MB, Semple MN. 1995. Monaural inhibition in cat auditory cortex. J Neurophysiol. 73:1876–1891.

Carney LH, Yin TC. 1988. Temporal coding of resonances by low-frequency auditory nerve fibers: single-fiber responses and a population model. J Neurophysiol. 60:1653–1677.

Cheung SW, Nagarajan SS, Bedenbaugh PH, Schreiner CE, Wang X, Wong A. 2001. Auditory cortical neuron response differences under isoflurane versus pentobarbital anesthesia. Hear Res. 156:115–127.
Contreras D. 2007. Propagating waves in visual cortex. Neuron. 55:3–5.
Delaney KR, Gelperin A, Fee MS, Flores JA, Gervais R, Tank DW, Kleinfeld D. 1994. Waves and stimulus-modulated dynamics in an oscillating olfactory network. Proc Natl Acad Sci U S A. 91:669–673.
Derdikman D, Hildesheim R, Ahissar E, Arieli A, Grinvald A. 2003. Imaging spatiotemporal dynamics of surround inhibition in the barrels somatosensory cortex. J Neurosci. 23:3100–3105.
Ermentrout GB, Kleinfeld D. 2001. Traveling electrical waves in cortex: insights from phase dynamics and speculation on a computational role. Neuron. 29:33–44.
Franks NP. 2008. General anaesthesia: from molecular targets to neuronal pathways of sleep and arousal. Nat Rev Neurosci. 9:370–386.
Freo U, Ori C. 2004. Effects of anesthesia and recovery from ketamine racemate and enantiomers on regional cerebral glucose metabolism in rats. Anesthesiology. 100:1172–1178.
Gourévitch B, Eggermont JJ. 2007. Evaluating information transfer between auditory cortical neurons. J Neurophysiol. 97:2533–2543.
Harrison RV, Harel N, Hamrahi H, Panesar J, Mori N, Mount RJ. 2000. Local haemodynamic changes associated with neural activity in auditory cortex. Acta Otolaryngol. 120:255–258.
Hess A, Scheich H. 1996. Optical and FDG mapping of frequency-specific activity in auditory cortex. Neuroreport. 7:2643–2647.
Hevers W, Hadley SH, Lüddens H, Amin J. 2008. Ketamine, but not phencyclidine, selectively modulates cerebellar GABA(A) receptors containing alpha6 and delta subunits. J Neurosci. 28:5383–5393.
Kalatsky VA, Polley DB, Merzenich MM, Schreiner CE, Stryker MP. 2005. Fine functional organization of auditory cortex revealed by Fourier optical imaging. Proc Natl Acad Sci U S A. 102:13325–13330.
Kayama Y, Iwama K. 1972. The EEG, evoked potentials, and single-unit activity during ketamine anesthesia in cats. Anesthesiology. 36:316–328.
Kral A, Tillein J, Hubka P, Schiemann D, Heid S, Hartmann R, Engel AK. 2009. Spatiotemporal patterns of cortical activity with bilateral cochlear implants in congenital deafness. J Neurosci. 29:811–827.
Kubota M, Sugimoto S, Horikawa J, Nasu M, Taniguchi I. 1997. Optical imaging of dynamic horizontal spread of excitation in rat auditory cortex slices. Neurosci Lett. 237:77–80.
Lee CC, Winer JA. 2008a. Connections of cat auditory cortex: I. Thalamocortical system. J Comp Neurol. 507:1879–1900.
Lee CC, Winer JA. 2008b. Connections of cat auditory cortex: III. Corticocortical system. J Comp Neurol. 507:1920–1943.
Manninen PH, Lam AM, Nicholas JF. 1985. The effects of isoflurane and isoflurane-nitrous oxide anesthesia on brainstem auditory evoked potentials in humans. Anesth Analg. 64:43–47.
Mansbach RS. 1991. Effects of NMDA receptor ligands on sensorimotor gating in the rat. Eur J Pharmacol. 202:61–66.
Massopust LC, Jr., Wolin LR, Albin MS. 1972. Electrophysiologic and behavioral responses to ketamine hydrochloride in the Rhesus monkey. Anesth Analg. 51:329–341.
McMullen NT, Velenovsky DS, Holmes MG. 2005. Auditory thalamic organization: cellular slabs, dendritic arbors and tectothalamic axons underlying the frequency map. Neuroscience. 136:927–943.
Narimatsu E, Kawamata Y, Kawamata M, Fujimura N, Namiki A. 2002. NMDA receptor-mediated mechanism of ketamine-induced facilitation of glutamatergic excitatory synaptic transmission. Brain Res. 953:272–275.
Nelken I. 2004. Processing of complex stimuli and natural scenes in the auditory cortex. Curr Opin Neurobiol. 14:474–480.
Nelken I, Bizley JK, Nodal FR, Ahmed B, King AJ, Schnupp JW. 2008. Responses of auditory cortex to complex stimuli: functional organization revealed using intrinsic optical signals. J Neurophysiol. 99:1928–1941.
Nowak LG, Bullier J. 1998. Axons, but not cell bodies, are activated by electrical stimulation in cortical gray matter. I. Evidence from chronaxie measurements. Exp Brain Res. 118:477–488.
Ojima H, Takayanagi M, Potapov D, Homma R. 2005. Isofrequency band-like zones of activation revealed by optical imaging of intrinsic signals in the cat primary auditory cortex. Cereb Cortex. 15:1497–1509.
Ori C, Dam M, Pizzolato G, Battistin L, Giron G. 1986. Effects of isoflurane anesthesia on local cerebral glucose utilization in the rat. Anesthesiology. 65:152–156.
Oye I, Paulsen O, Maurset A. 1992. Effects of ketamine on sensory perception: evidence for a role of N-methyl-D-aspartate receptors. J Pharmacol Exp Ther. 260:1209–1213.
Petersen CC, Grinvald A, Sakmann B. 2003. Spatiotemporal dynamics of sensory responses in layer 2/3 of rat barrel cortex measured in vivo by voltage-sensitive dye imaging combined with whole-cell voltage recordings and neuron reconstructions. J Neurosci. 23:1298–1309.
Polley DB, Read HL, Storace DA, Merzenich MM. 2007. Multiparametric auditory receptive field organization across five cortical fields in the albino rat. J Neurophysiol. 97:3621–3638.
Prechtl JC, Bullock TH, Kleinfeld D. 2000. Direct evidence for local oscillatory current sources and intracortical phase gradients in turtle visual cortex. Proc Natl Acad Sci U S A. 97:877–882.
Prechtl JC, Cohen LB, Pesaran B, Mitra PP, Kleinfeld D. 1997. Visual stimuli induce waves of electrical activity in turtle cortex. Proc Natl Acad Sci U S A. 94:7621–7626.
Read HL, Winer JA, Schreiner CE. 2002. Functional architecture of auditory cortex. Curr Opin Neurobiol. 12:433–440.
Roland PE, Hanazawa A, Undeman C, Eriksson D, Tompa T, Nakamura H, Valentiniene S, Ahmed B. 2006. Cortical feedback depolarization waves: a mechanism of top-down influence on early visual areas. Proc Natl Acad Sci U S A. 103:12586–12591.
Rouiller EM, Simm GM, Villa AE, de Ribaupierre Y, de Ribaupierre F. 1991. Auditory corticocortical interconnections in the cat: evidence for parallel and hierarchical arrangement of the auditory cortical areas. Exp Brain Res. 86:483–505.
Rubino D, Robbins KA, Hatsopoulos NG. 2006. Propagating waves mediate information transfer in the motor cortex. Nat Neurosci. 9:1549–1557.
Sally SL, Kelly JB. 1988. Organization of auditory cortex in the albino rat: sound frequency. J Neurophysiol. 59:1627–1638.
Santarelli R, Arslan E, Carraro L, Conti G, Capello M, Plourde G. 2003. Effects of isoflurane on the auditory brainstem responses and middle latency responses of rats. Acta Otolaryngol. 123:176–181.
Santarelli R, Carraro L, Conti G, Capello M, Plourde G, Arslan E. 2003. Effects of isoflurane on auditory middle latency (MLRs) and steady-state (SSRs) responses recorded from the temporal cortex of the rat. Brain Res. 973:240–251.
Schreiner CE, Winer JA. 2007. Auditory cortex mapmaking: principles, projections, and plasticity. Neuron. 56:356–365.
Sebel PS, Ingram DA, Flynn PJ, Rutherfoord CF, Rogers H. 1986. Evoked potentials during isoflurane anaesthesia. Br J Anaesth. 58:580–585.
Senseman DM, Robbins KA. 1999. Modal behavior of cortical neural networks during visual processing. J Neurosci. 19:RC3.
Shamma SA, Symmes D. 1985. Patterns of inhibition in auditory cortical cells in awake squirrel monkeys. Hear Res. 19:1–13.
Sharon D, Grinvald A. 2002. Dynamics and constancy in cortical spatiotemporal patterns of orientation processing. Science. 295:512–515.
Shaw NA. 1988. The auditory evoked potential in the rat—a review. Prog Neurobiol. 31:19–45.
Shaw NA. 1990. Central auditory conduction time in the rat. Exp Brain Res. 79:217–220.
Song WJ, Kawaguchi H, Totoki S, Inoue Y, Katura T, Maeda S, Inagaki S, Shirasawa H, Nishimura M. 2006. Cortical intrinsic circuits can support activity propagation through an isofrequency strip of the guinea pig primary auditory cortex. Cereb Cortex. 16:718–729.
Sutter ML, Schreiner CE, McLean M, O'Connor KN, Loftus WC. 1999. Organization of inhibitory frequency receptive fields in cat primary auditory cortex. J Neurophysiol. 82:2358–2371.
Takahashi H, Nakao M, Kaga K. 2005. Interfield differences in intensity and frequency representation of evoked potentials in rat auditory cortex. Hear Res. 210:9–23.
Thiel A, Russ W, Hempelmann G. 1988. [Evoked potentials and inhalation anesthetics]. Klin Wochenschr. 66(Suppl 14):11–18.

Thornton C, Creagh-Barry P, Jordan C, Luff NP, Dore CJ, Henley M, Newton DE. 1992. Somatosensory and auditory evoked responses recorded simultaneously: differential effects of nitrous oxide and isoflurane. Br J Anaesth. 68:508–514.
Tsytsarev V, Fukuyama H, Pope D, Pumbo E, Kimura M. 2009. Optical imaging of interaural time difference representation in rat auditory cortex. Front Neuroengineering. 2:1–7.
Tsytsarev V, Premachandra K, Takeshita D, Bahar S. 2008. Imaging cortical electrical stimulation in vivo: fast intrinsic optical signal versus voltage-sensitive dyes. Opt Lett. 33:1032–1034.
Tsytsarev V, Tanaka S. 2002. Intrinsic optical signals from rat primary auditory cortex in response to sound stimuli presented to contralateral, ipsilateral and bilateral ears. Neuroreport. 13:1661–1666.
Tsytsarev V, Yamazaki T, Ribot J, Tanaka S. 2004. Sound frequency representation in cat auditory cortex. Neuroimage. 23:1246–1255.
Velenovsky DS, Cetas JS, Price RO, Sinex DG, McMullen NT. 2003. Functional subregions in primary auditory cortex defined by thalamocortical terminal arbors: an electrophysiological and anterograde labeling study. J Neurosci. 23:308–316.
Versnel H, Mossop JE, Mrsic-Flogel TD, Ahmed B, Moore DR. 2002. Optical imaging of intrinsic signals in ferret auditory cortex: responses to narrowband sound stimuli. J Neurophysiol. 88:1545–1558.
Wei H, Liang G, Yang H, Wang Q, Hawkins B, Madesh M, Wang S, Eckenhoff RG. 2008. The common inhalational anesthetic isoflurane induces apoptosis via activation of inositol 1,4,5-trisphosphate receptors. Anesthesiology. 108:251–260.
Winer JA, Lee CC. 2007. The distributed auditory cortex. Hear Res. 229:3–13.
Wong DH, Jenkins LC. 1974. An experimental study of the mechanism of action of ketamine on the central nervous system. Can Anaesth Soc J. 21:57–67.
Xu W, Huang X, Takagaki K, Wu JY. 2007. Compression and reflection of visually evoked cortical waves. Neuron. 55:119–129.